Mini Review on PEDOT:PSS as a Conducting Material in Energy Harvesting and Storage Devices Applications

HYUNGSUB YOON[a*], HEEBO HA[a], CHUNGHYEON CHOI[a],
TAE GWANG YUN[b] AND BYUNGIL HWANG[a]

[a]*School of Integrative Engineering, Chung-Ang University, Seoul 06974, Republic of Korea*

[b]*Department of Materials Science and Engineering, Myongji University, Yongin, Gyeonggi 17058, Republic of Korea*

ABSTRACT

Poly(3,4-ethylenedioxythiophene):polystyrene sulfonate (PEDOT:PSS), one of the conducting polymers, is widely used as a conducting material in various applications. PEDOT:PSS possesses high electrical conductivity, optical transparency in visible light range, good chemical and physical stability in ambient state, etc. Furthermore, PEDOT:PSS offers the advantages of flexibility and possibility of solution-based process, which makes it suitable for use in flexible electronic devices. In this mini review, the applications of PEDOT:PSS as a conductive parts in energy harvesting and storage technologies are discussed and summarized.

KEYWORDS*: PEDOT:PSS, Electrode, Energy harvesting, Energy storage, Stability.*

1. INTRODUCTION

With the development of the Internet-of-things (IOT), wearable devices such as smart watches and health-sensing devices have attracted tremendous attention from researchers [1-8]. The materials used to fabricate wearable devices should possess stable mechanical properties in various deformation environments depending on human movement [9-15]. From this perspective, conducting polymers are considered suitable alternatives to rigid materials. In addition to flexibility, conducting polymers can transport electrons owing to their π-conjugated structures. There are various types of conducting polymers such as polyaniline (PANi), polypyrrole (PPy), and poly(3,4-ethylenedioxythiophene): poly (styrenesulfonate) (PEDOT:PSS)[16-19]. Especially, PEDOT:PSS, which is a combination of

J. Polym. Mater. Vol. **40,** No. 1-2, 2023, 1-17

*Correspondence author e-mail: bihwang@cau.ac.kr, ytk0402@mju.ac.kr
DOI : https://doi.org/10.32381/JPM.2023.40.1-2.1

positively charged PEDOT and negatively charged PSS held together by Coulombic forces, has high electrical conductivity, optical transparency in the visible range, and flexibility. Moreover, it can be processed using the solution process because of its solubility in water. The property of being well dispersed in water increased the application range of PEDOT:PSS because of ease to fabricate films or composites. The chemical structure of PEDOT:PSS is shown in Figure 1. In addition, electrical conductivity can be improved easily up to four times through a treatment called 'secondary dopant'. If it is carried out using ethylene glycol (EG) and dimethyl sulfoxide (DMSO), acid and alcohol, enhanced characteristics continue even after the secondary dopant is completely removed, and it can be applied to various applications [20]. Therefore, PEDOT:PSS is used as an active

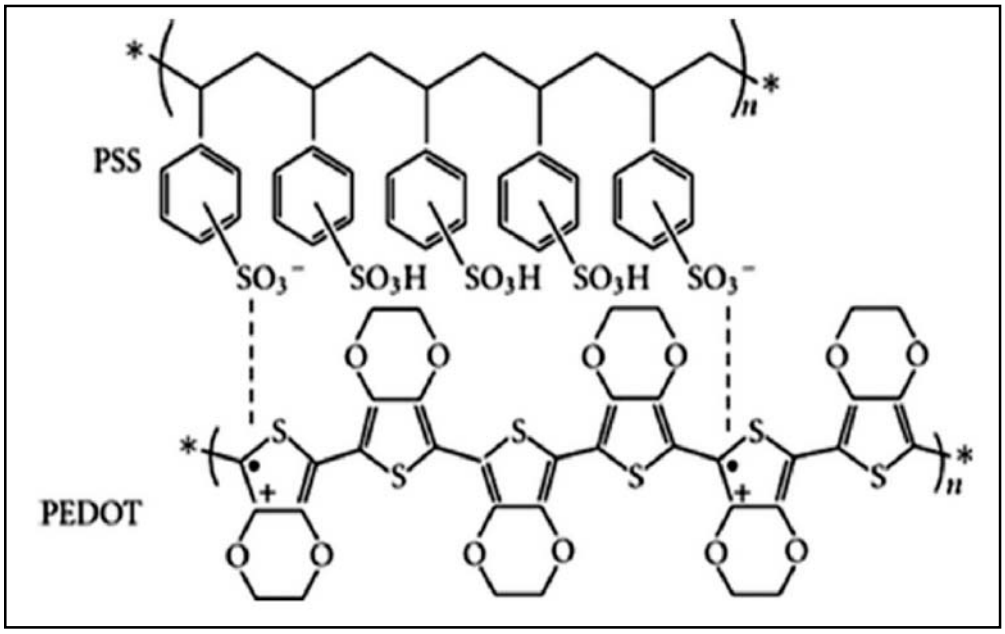

Fig. 1. Chemical structure of PEDOT:PSS

material in diverse fields. In this paper, we review studies wherein PEDOT:PSS has been used as an active material in energy harvesting and storage systems.

2. Application to Thermoelectric Devices

Thermoelectric (TE) devices are one of energy harvesting systems and can generate electricity by using the heat of human skin for wearable electronics[21]. It can be used in wearable devices to ensure a continuous supply of electricity. In general, the performance of thermoelectric devices is rated using a dimensionless Figure-of-merit (ZT), which is expressed as $ZT = S^2\sigma T/k$, where S is Seebeck coefficient, σ is electrical conductivity, T is the

absolute temperature, and k is thermal conductivity or power factor (PF = $S^2\sigma$). According to the above equation of ZT, the performance of thermoelectric devices can be improved by using materials that possess a high level of electrical conductivity and low level of thermal conductivity.

Although researches using inorganic materials are being conducted to achieve the high efficiency of TE devices, organic materials such as PPy, PANI and PEDOT:PSS have advantages such as eco-friendly, low cost, high flexibility, high electrical conductivity, and low thermal conductivity[20]. Among organic materials, PEDOT:PSS exhibits high electrical conductivity through doping, and is widely used in organic TE device research [22]. However, if only organic material is used, it shows the low PF value [23]. This requires solution to improve the low Seebeck coefficient that can be achieved by fermi level moving. As one of the approaches, studies are being conducted to mix carbon materials together with organic materials. Through the reaction of PEDOT:PSS and chemicals such as EG and DMSO, electrical conductivity and ZT could be improved due to a large specific surface area and high electrical conductivity of carbon materials by mixing with PEDOT:PSS and carbon materials [24, 25]. In addition, it has high carrier mobility and is suitable for TE devices as it is an interaction that lowers thermal conductivity by coating carbon materials with organic materials.

For example, Kim et al., [26]. demonstrated the electrical conductivity of ~620 S/cm and the power factor performance of ~33 $\mu W/m{\cdot}K^2$ for PEDOT:PSS treated by DMSO. Also, Yu et al.,[27] mixed single walled carbon nanotube (SWCNT) and PEDOT:PSS. High electrical conductivity of 1000 S/cm and high PF value of 160 $\mu W/m{\cdot}K^2$ were shown by the doping of PEDOT and high electrical conductivity of SWCNT using DMSO. Electrical conductivity of ~654 S/cm and PF of ~133 $\mu W/m{\cdot}K^2$ were shown by a mixture of MWCNT and EG-treated PEDOT[25]. The electrical conductivity of PEDOT:PSS was improved by unchaining of PSS using EG, and it showed the possibility to apply TE devices by mixing CNT and treated-PEDOT:PSS. In the case of SWCNT, it had high electrical conductivity, showing a higher PF value than MWCNT.

Xiong et al.,[24] showed that the composite using graphene and PEDOT:PSS has the advantages of graphene's unique two-democratic structure, high electrical conductivity, and high carrier mobility, and shows relatively high electrical conductivity and PF of 637 S/cm and ~45.67 PF. This result demonstrated the applicability to TE devise using the PEDOT:PSS/carbon materials composites. However, the PEDOT:PSS based composite using the overall carbon material showed low values for the electrical conductivity and PF to be used in TE devices, so it is necessary to improve them.

Therefore, hybrid-type studies that complement low PF and use PEDOT:PSS and inorganic materials with the advantages of organic materials are in the spotlight. Inorganic materials based on Se or Te (AgSe, Bl_2Te_3, SnSe, Cu_2SnSE_3) showing high Seebeck coefficient are made of particles or nanowire (NW). And then, PEDOT:PSS coated particle and NW are made to the composites, which have high Seebeck coefficient and low thermal conductivity, and also ensures flexibility by the organic materials.

Kato et al., [28] conducted a research on hybrid TE film using $CoSb_{3-x}Te_x$ and PEDOT:PSS. It has suitable Seebeck coefficient as it could quickly increase Seebeck coefficient by doping $CoSb_3$ using Te to increase carrier concentration. The $CoSb_{3-x}Te_x$ material was broken into small powder through grinding and ball-milling, dispersed in a PEDOT:PSS/DMSO solution, and the films were obtained by vacuum filtration [Figure 2 (a)]. Although very high Seebeck coefficient according to $CoSb_{3-x}Te_x$ weight fraction was shown and

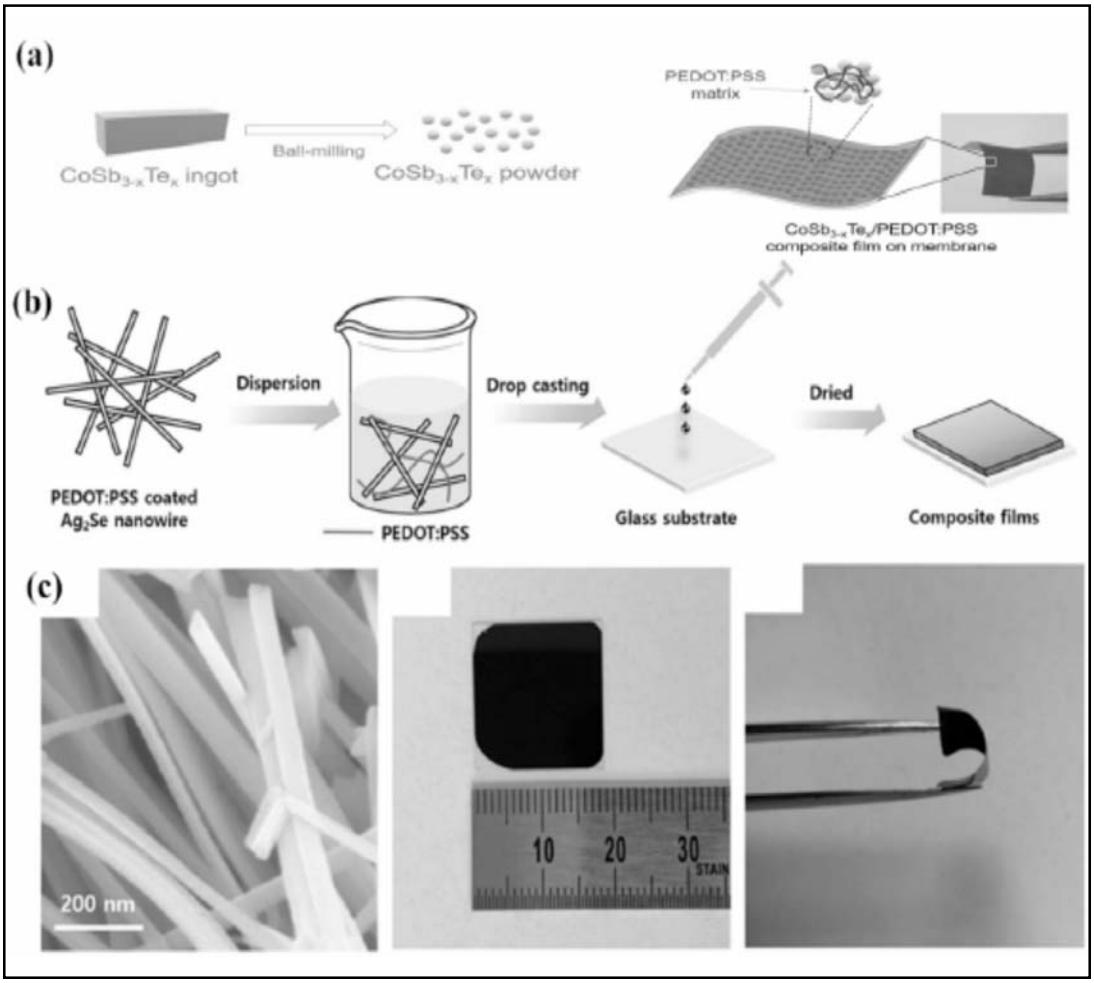

Fig. 2. (a) Schematic diagram of composite film. Reprinted from[28] under the Creative Commons Attribution 4.0 International (CC BY 4.0) License). (b) schematic diagram of the preparation process for the PEDOT:PSS-coated Ag_2Se NW/PEDOT:PSS composite films. (c) FE-SEM image and Digital photo image of Ag_2Se NW/PEDOT:PSS composite films. Reprinted from [29, 30] under the Creative Commons Attribution 4.0 International (CC BY 4.0) License).

PF was very low due to very low electrical conductivity [28].

Park et al., [30] produced a composite film using Ag_2Se NW and PEDOT:PSS. Pre-treated PEDOT:PSS was coated on Ag_2Se NW using DMSO to manufacture a flexible film through a simple drop-casting method [Figure 2 (b)]. As shown in Figure 2 (c), it showed that the Ag_2Se/PEDOT:PSS composite could be used in flexible TE devices. Thermoelectric properties showed a high PF of 327.15 $\mu W/m \cdot K^2$, which is about 25 times than the PF of pure PEDOT:PSS film and showed a high PF value compared to carbon materials. In addition, high electrical conductivity of 700 S/cm or more was also confirmed. When durability was checked by the bending test, it was represented that a decrease of ~5.9% after 1000 cycles, and it showed a good durability. This result demonstrated its applicability to flexible TE devices using PEDOT:PSS/Ag_2Se composites. However, when using this hybrid type composite, it is possible to produce it at a lower price than the existing inorganic, but there are still limitations because expensive fillers must be used.

3. Application to Perovskite Solar Cell

The photovoltaic (PV) solar cell technology uses sunlight to convert electricity, which is an infinite clean energy. Currently, commercialized PV solar cells are silicon-based. Silicon-based inorganic solar cells showed very excellent power conversion efficiency (PCE) and durability with advantages such as smooth surface morphology and high carrier mobility.

The efficiency of a solar cell is determined by the PCE. The equation of PCE is as follow [31]:

$$PCE\ (\eta) = \frac{J_{sc} \cdot V_{oc} \cdot FF}{P_{in}}$$

where the short-circuit current (J_{sc}) is the current flowing when there is no external field, the open-circuit voltage (V_{oc}) is the maximum voltage a solar cell can produce when no current flows, the fill factor (FF) is the value of multiplying the current and voltage at the maximum power point divided by multiplying V_{oc} and J_{sc}, and P_{in} is the power of light entering into the solar cell.

Silicon-based solar cells have high PCE (>20%) than organic solar cells, but they are heavy and brittle to use in flexible devices. Organic solar cells have less PCE than inorganic solar cells due to their low carrier mobility, but they are lightweight, high mechanical flexibility, semitransparent, excellent thermal stability and can be manufactured by solution process in a large area. Among them, the perovskite solar cell has an absorbance coefficient and optical properties of 10 times or more compared to other photoactive materials. In addition, there is an advantage in that the band gap may be easily tuned by changing the type of the halogen element of perovskite material structure (ABX_3) [32].

In perovskite solar cell, PEDOT:PSS is one of the most suitable materials for hole transport layer (HTL). In general, solar cells using organic materials have many durability problems that are vulnerable to moisture and oxygen. In the case of PEDOT:PSS, the structural stability of perovskite solar cells can be improved through tailoring PEDOT:PSS HTL using the doping methods through EG or DMSO and post-treatment methods [33].

Also, PEDOT:PSS has excellent electrical conductivity, high work function and good light

transmittance. It is also very suitable for use in HTL layers because it has a similar bandgap to materials such as ITO and ZTO used in flexible and semi-transparent solar cells. The electrical conductivity can be adjusted according to the synthesis method or the type of additive. Also, organic materials can be used to various solution-based coating methods such as spin coating and inkjet methods which are advantageous for large-area manufacturing.

Ali et al., [34] reported PCE changes by grain size of $Ti_3C_2T_x$ (MXene)-doped PEDOT:PSS as HTL. A research was conducted on the grain size of the active layer in which the perovskite material was deposited in accordance with the doped amount of MXene. The PCE depends mainly on various factors, such as work function, conductivity of charge-transport layers, chemical composition of perovskites, energy level alignment, bandgap, defects, and particle size. In inverted perovskite solar cells (PSCs), the HTL interface has a significant impact on the operational stability of the PSCs, which plays an important role in determining the PCE. In addition, it has been reported that the hydrophilicity and wettability of HTL affect the particle size of the $MAPbI_3$ layer, increasing the conductivity, and thus becoming a device with a higher PCE. Figure 3 (a) showed the morphology of $MAPbI_3$ layer and grain size distribution [insets of Figure 3 (a)] as an active layer on HTL using MXene/PEDOT:PSS. Before MXene was added [left of Figure 3 (a)], the grain size of ~250 nm was shown, and when 0.03 wt.% of MXene was added [right of Figure 3 (a)], it showed that the grain size was increased to ~400 nm. PCE, J_{sc}, FF, and V_{oc} increased according to doping concentrations and all results increased as the grain size of the $MAPbI_3$ increased [34]. This result demonstrated the change in PCE according to the morphology in the active layer.

As another study, Jung et al., [35] reported the efficiency of PEDOT:PSS/additive (Brij C10) mixed HTL as shown in Figure 3 (b). According to additives concentration, PEDOT:PSS/3 wt.%-additive mixed HTL showed best performance in J_{sc}, V_{oc}, FF and PCE [35]. As mentioned above, we talked about the effect of the change in grain size, that is, morphology change. However, as shown in Figure 3 (c), when only PEDOT:PSS was used, it had the largest grain size. The grain size decreases as the concentration of the additive increases. In general, larger perovskite grains have higher efficiency through superior charge transport, lower trap density, and reduced bulk recombination. However, the steady-state and time-resolved PL results showed that non-radiative recombination was reduced at the interface of HTL, and the suppressed recombination improved PCE despite the grain size reduction of the perovskite layer [35]. These results represented that not only grain size, but also other conditions are important, and demonstrate the importance of mixture research using PEDOT:PSS on HTL.

In addition to these researches, study that increased the PCE efficiency from 13.2% to 15.3% even though the grain size was reduced using GO-doped PEDOT:PSS as HTL, and study that increased the PCE efficiency from 11.9% to 14.2% using CuSCN-doped PEDOT:PSS were also reported [36, 37]. Many studies have been published to increase the PCE of PSC through doped PEDOT:PSS, and a solution process suitable for a large area is

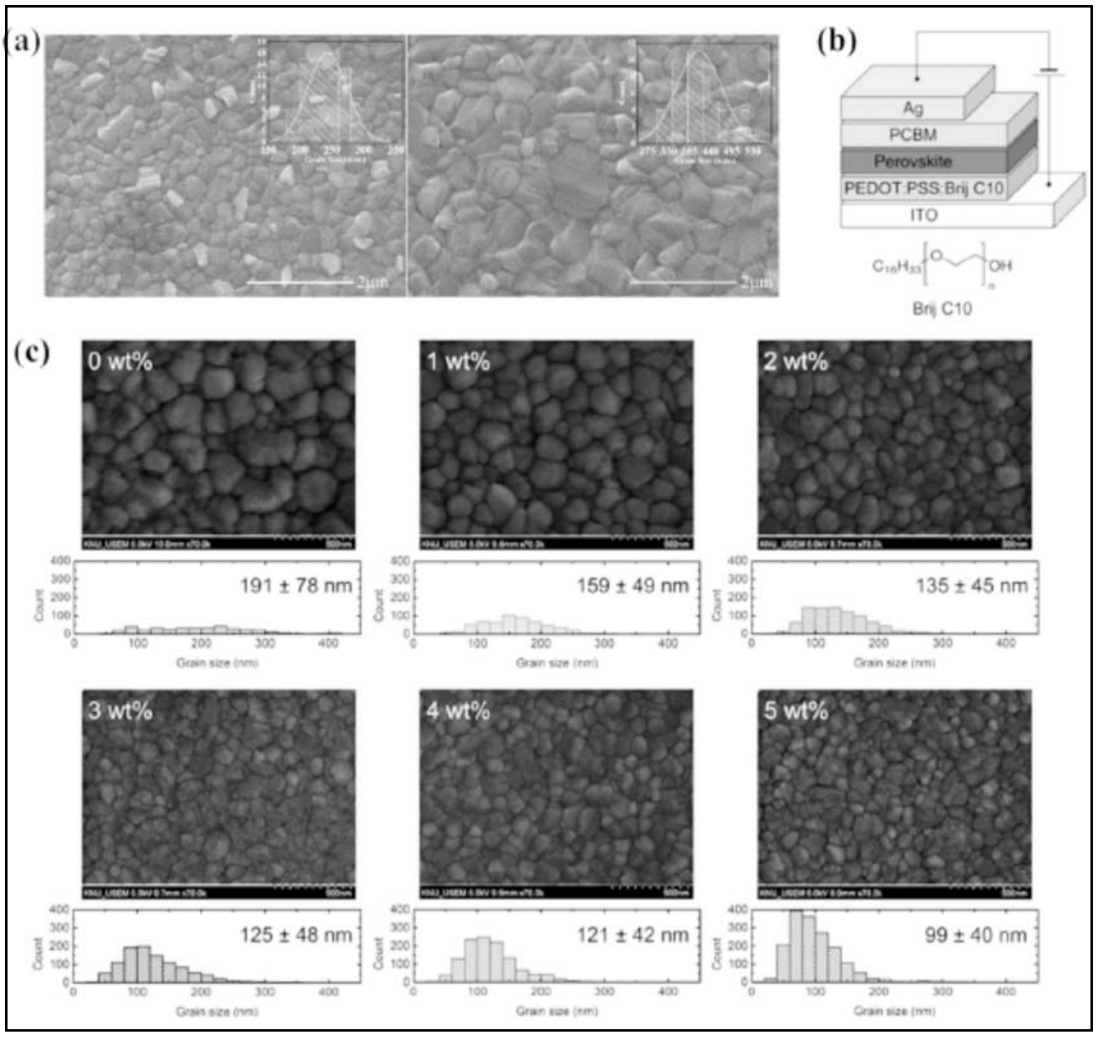

Fig. 3. (a) SEM images of perovskite films deposited over PEDOT:PSS with $Ti_3C_2T_x$ doping concentrations of 0 wt.%, 0.03 wt.%. Reprinted from [34] under the Creative Commons Attribution 4.0 International (CC BY 4.0) License). (b) Device structure of PSCs and chemical structure of Brij C10. (c) Top-view SEM images of perovskite film on Brij C10-modified (0, 1, 2, 3, 4, and 5 wt.%) and statistics of grain size. Reprinted from [35] under the Creative Commons Attribution 4.0 International (CC BY 4.0) License).

possible compared to silicon-based solar cells, but it still needs to be improved the PCE and durability by oxygen and moisture.

4. Application as Supercapacitor

Supercapacitors have been considered as one of the promising energy sources for wearable

devices and automotive applications [38-43]. In general, the supercapacitor can be categorized as electrical double layer capacitors (EDLCs) and pseudocapacitors. The carbonaceous materials such as active carbon, graphene, carbon nanotubes, etc. are used as active materials of the EDLCs. Although the EDLCs have high power density and good cyclic stability, they show low energy density because energy storage occurs on the surface of active materials via adsorption and desorption of ions. To deal with the low energy density of EDLCs, the pseudocapacitor, which storages energy via redox reactions between active materials and ions of electrolytes, can enhance the energy density and specific capacitance of the capacitors. Transition metal oxides such as TiO_2, RuO_2, etc. and conducting polymers are widely used as active materials of pseudocapacitor. Especially, PEDOT:PSS has been widely used because of high electrical conductivity, ease of hybridization with other materials, solution-based processability and good stability in ambient state.

Ko et al.,[44] fabricated cellulose/PEDOT:PSS based supercapacitor and proved the effect of post treatment on the capacitance of the devices. They selected the polar solvents such as DMSO and EG for post treatment which can improve the electrical conductivity of the PEDOT:PSS by rearranging the PEDOT:PSS chains and removing the excess PSS parts which are an insulator. The cellulose nanofibers (CNFs)/PEDOT:PSS mixture solution was filtered through the vacuum assisted filtration, and they dropped the polar solvents on the surface of the film for treatment process. The PEDOT:PSS/CNF film was peeled off after drying, as shown in Figure 4 (a). The values of electrical conductivity were 123.37, 106.6, and 1.05 S/cm for DMSO treated, EG treated, and pure PEDOT:PSS/CNF films, respectively. They measured electrochemical performance using 0.5M H_2SO_4 as electrolyte through three electrode system. At 2 mV/s of scan rate, the cyclic voltammetry [44] graphs of the films with post treatment showed the increased current and enlarged area compared to the films without the treatment [44]. In the galvanostatic charge-discharge (GCD) curves, the films with treatment showed longer discharge time, and the calculated capacitances from GCD curves were 25, 22, 20 F/g at current density of 0.1 A/g, corresponding to EG treated, DMSO treated, and pure PEDOT:PSS/CNF film, respectively[44]. This results indicated the organic solvent treatment enhanced the electrical conductivity and the electrochemical performance of PEDOT:PSS composite by removal of PSS part and rearrangement of PEDOT chains.

In the work of Liu et al., [45], they fabricated free-standing graphene/PEDOT:PSS films as electrodes for supercapacitors through a bar coating. They used diethylene glycol [45] as a secondary dopant and used hypophosphorous acid as a reducing agent of the GO. The resulted films and orthophosphoric acid /poly (vinyl alcohol) (H_3PO_4/PVA) gel electrolyte were sandwiched to make all-solid-state symmetric supercapacitor [Figure 4 (b)]. The rGO-PEDOT:PSS based supercapacitor exhibited much higher current and larger area compared to the other materials based supercapacitors, indicating a faster charge transfer and higher capacitance of rGO-PEDOT:PSS based supercapacitor [45]. The maximum power density and energy density were 159.8 W/kg and 1.95

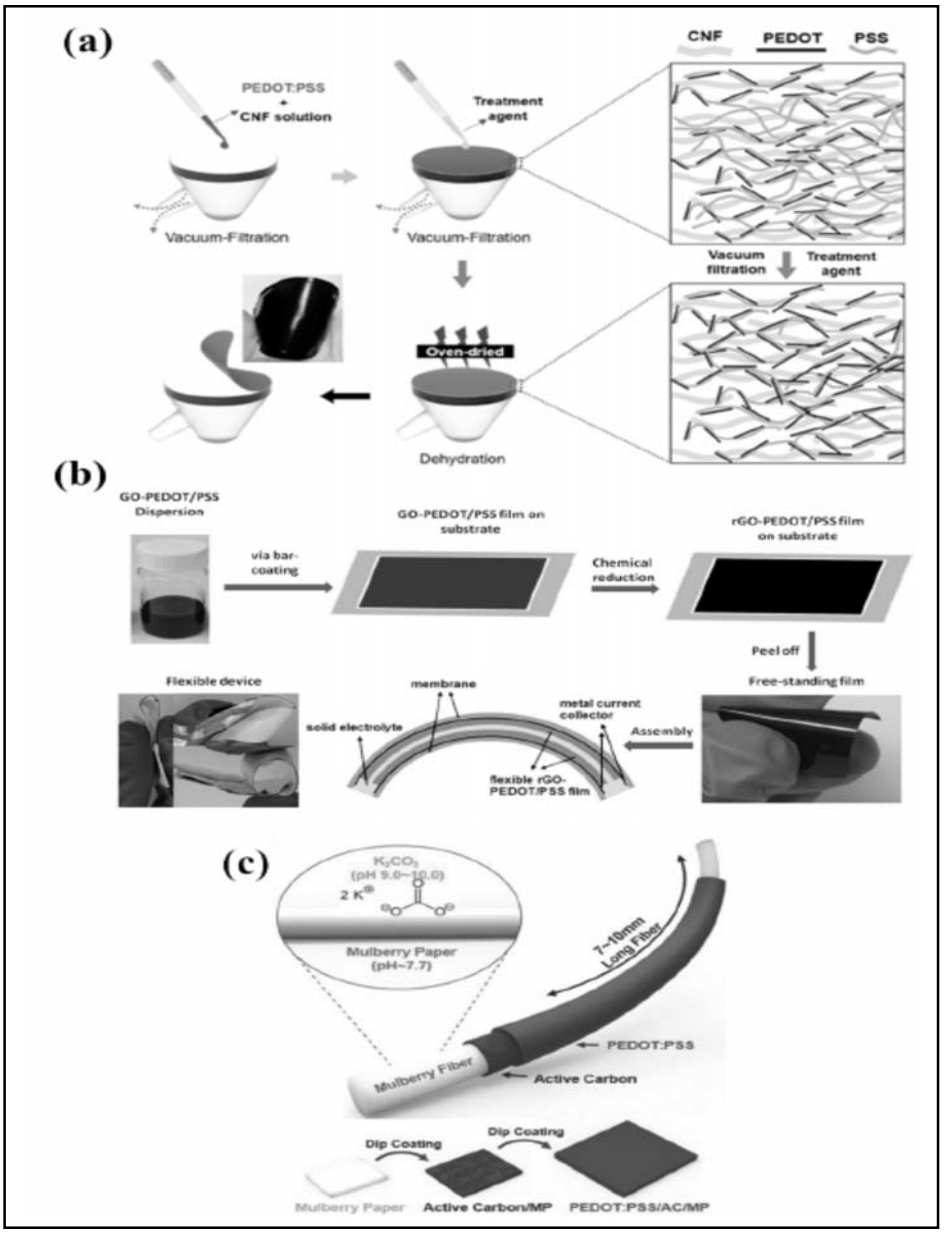

Fig. 4. (a) Illustration of the fabrication process of PEDOT:PSS/CNF film. Reprinted from [44] under the Creative Commons Attribution 4.0 International (CC BY 4.0) License). (b) Preparation process of rGO-PEDOT:PSS films and rGO-PEDOT:PSS based supercapacitor. Reprinted from [45] under the Creative Commons Attribution 4.0 International (CC BY 4.0) License). (c) Schematic illustration of mulberry paper based supercapacitor. Reprinted from [46]. Copyright 2018 Wiley.

Wh/kg for pure rGO based supercapacitor, 1,967.5 W/kg and 1.00 Wh/kg for pure PEDOT:PSS based supercapacitor, and 3,589.5 W/kg and 2.83 Wh/kg for rGO-PEDOT:PSS based supercapacitor[45]. The results proved that the hybridization of rGO and PEDOT:PSS was effective method on enhancing the electrochemical performance of the supercapacitors. Under various bending degrees and many cycles of bending, there was negligible difference in CV curves of rGO-PEDOT:PSS based supercapacitors, indicating the fabricated supercapacitor was suitable for flexible application[45].

In the work of Yun et al.,[46], the mulberry paper (MP) based supercapacitor was prepared by coating active carbon (AC) and PEDOT:PSS as active materials. The mulberry paper has been considered as promising substrate for flexible supercapacitor with outstanding mechanical and chemical properties. Furthermore, due to the hydrophilicity of the paper, the simple dip coating method can be used to coat the active materials, which enables high loading of active materials in aqueous based process [Figure 4 (c)]. Compared to the GCD profiles of MP/AC, the discharge time of MP/AC/PEDOT:PSS showed longer, indicating the addition of PEDOT:PSS as the active material is beneficial for the supercapacitor with higher specific capacitance[46]. The specific capacitances of MP/AC and MP/AC/PEDOT:PSS from GCD curves at 1 A/g of current density were 147 F/g and 374 F/g, respectively[46]. Furthermore, the specific capacitances of MP/AC/PEDOT:PSS at 32 A/g of current density can be maintained 93% of the capacitance at 1 A/g. But the capacitance of MP/AC at 32 A/g was 87 % of the capacitance at 1 A/g[46]. Although the cycle stability of MP/AC after 15,000 cycles at 1 A/g of current density were maintained 96.9% of initial capacitance, which is better than that of MP/AC/PEDOT:PSS, the MP/AC/PEDOT:PSS also showed outstanding cyclic stability as 90.7% of initial capacitance [46]. After repeated charge-discharge test, the PEDOT:PSS was detached from the electrode, which can be factor of decrease in cyclic stability. The research on enhancing the bonding strength between PEDOT:PSS and substrate will be required to fabricate the supercapacitors with better performance. In this work, they demonstrated that the PEDOT:PSS is one of the promising and valuable candidates for enhancing the electrochemical performance of the supercapacitor.

Zhao et al.,[47] also utilized PEDOT:PSS and rGO as the active materials to fabricate flexible electrodes for use in supercapacitors. In general, pristine-rGO-based electrodes have low capacitance owing to accumulation of the rGO layer. However, by utilizing PEDOT:PSS, this shortcoming of rGO-based electrodes can be overcome. Furthermore, they suggested that PEDOT:PSS can be utilized to fabricate self-healing electrodes by means of steam treatment. To fabricate a self-healing supercapacitor, they deposited PEDOT:PSS and rGO on a polyurethane (PU)-based substrate and used a hydrogel electrolyte containing crosslinking materials with 2-ureido-4-pyrimidone (UPy) and lauryl functional groups. As shown in Figure 5 (a), they utilized acrylamide (AAm) and lauryl methacrylate (LMA) as the lauryl group agent and 4-(6-(3-(6-(4-methyl-4-oxa-1,4-dihydropyrimidin-2-yl) ureido) hexylcarbamoyloxy) butyl acrylate

(UPyHCBA) as the UPy group agent. Each crosslinking material was synthesized through copolymerization to prepare the hydrogel-type self-healing electrolyte, which can be crosslinked through hydrogen bonding when the electrolyte is broken [Figure 5 (b)]. When the fabricated PDOT:PSS and rGO electrode on the PU-based substrate were broken, the composite electrode healed under steam treatment [Figure 5 (c)]. Under steam treatment, the PSS chains of PEDOT:PSS captured water molecules, and therefore, the volume of the PSS part increased. The increased volume of the PSS part filled the broken site and restored the conductive path. Thus, owing to the synergistic effects of the hydrogel electrolyte and the PEDOT:PSS based electrode, the obtained supercapacitor exhibited self-healing behavior. Furthermore, the specific capacitance values of the fabricated

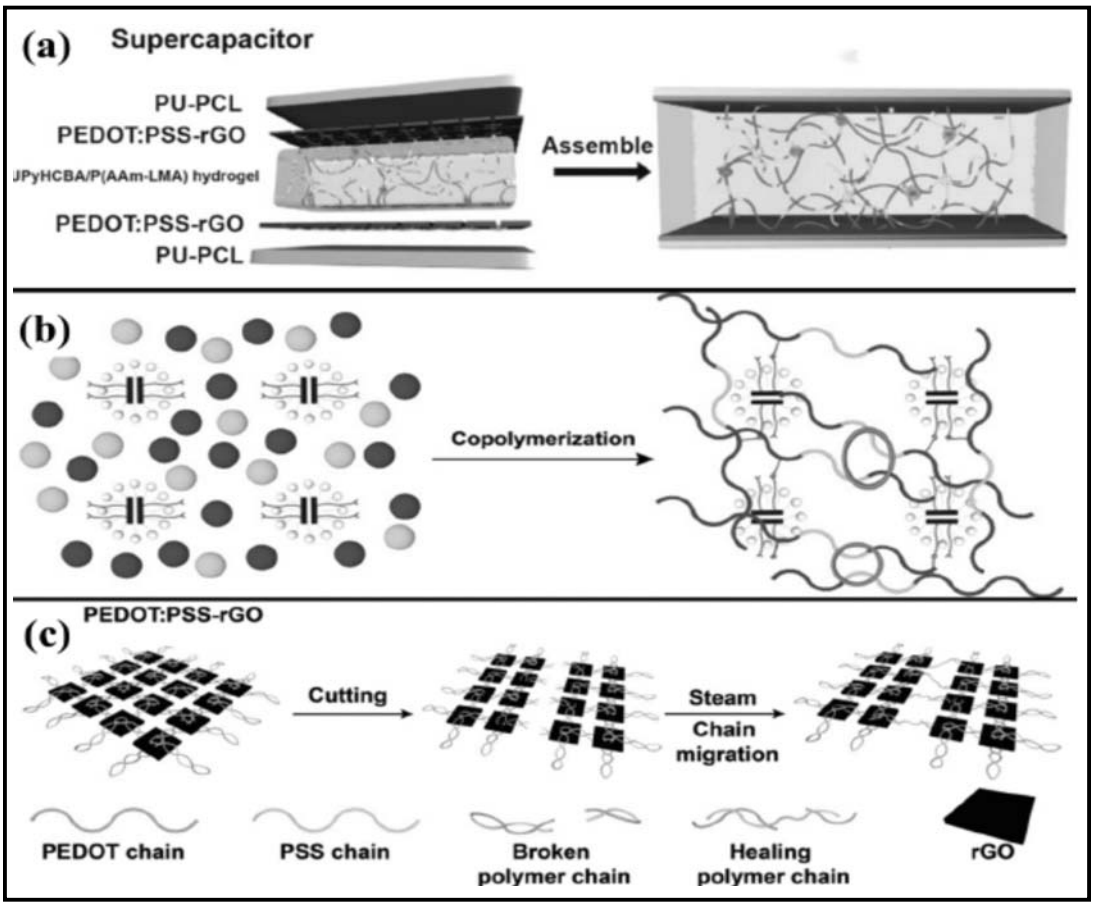

Fig. 5. (a) Illustrations of the self-healable PEDOT:PSS-rGO based supercapacitor, (b) diagrams of hydrogel electrolyte synthesis, (c) mechanism of the self-healing process of the PEDOT:PSS-rGO based supercapacitor. Reprinted from [47] under the Creative Commons Attribution 4.0 International (CC BY 4.0) License).

supercapacitor were 52.2 F/g and 38.0 F/g as calculated using the cyclic voltammetry curve at 10 mV/s and charge-discharge curve at 0.5 A/g, respectively[47]. Although the specific capacitance values were not high, the cyclic stability was excellent, and 95.8% of the initial capacitance was maintained after 10,000 cycles[47]. Furthermore, after five repeated cutting and healing cycles, the capacitance variation was negligible[47]. This result demonstrated the self-healing nature of the fabricated supercapacitor.

5. Application in Transpiration-driven Electrokinetic Power Generator (TEPG)

PEDOT:PSS can be applied to a transpiration-driven electrokinetic power generator (TEPG), which is new concept of energy harvesting technologies utilizing their high electrical conductivity and hydrophilicity properties. Because the TEPG device utilizes the abundant and eco-friendly water as an energy source for generating the power and energy, TEPG device has attracted the tremendous attention. The main concept of the TEPG is transpiration, whereby water is transported from the roots to the leaves in plants. Therefore, the hydrophilicity is essential property in TEPG device. Similar to plants, when the TEPG is wetted by dripping water on one of its sides, a water potential gradient is created and thus water flows from the wet side to the dry side. Through the phenomenon caused by the movement of water, TEPG devices can generate the electricity, which will be explained in detail below.

Yun et al., [48] used PEDOT:PSS as an active material to fabricate TEPG device. To fabricate the TEPG, they utilized a PEDOT:PSS dispersion the conductive materials and a cotton fabric as the substrate in the dipping process. The resistance of the TEPG was controlled by the changing the number of times the cotton substrate was dipped. The energy harvesting mechanisms of the PEDOT:PSS-coated TEPG (p-TEPG) are i) electrical double layer, ii) ion-permselectivity, and iii) capillary flow. At first, in the electrical double layer, when water is dropped on the TEPG, protons are absorbed on the surface of the PEDOT:PSS, which reduces the surface energy spontaneously because of the high surface energy of the PEDOT:PSS. In addition to the electrical double layer, because of the negatively charged PSS (SO_3^-) on the TEPG surface, cations and anions are attracted and repelled, respectively, when the electrolyte is dropped, which is called as ion-permselectivity [Figure 6 (a)]. Because of the charge densities resulting from the electrical double layer and ion-permselectivity, a steeper charge gradient is formed between the wet and dry sides. As a result, the TEPG device generates a voltage due to the electrical potential difference between the wet and dry sides. To further investigate the effect of ion-permselectivity of the PEDOT:PSS, they compared carbon-coated, PANi-coated (positively charged surface), PPy-coated (positively charged surface), and p-TEPG. The results, shown in Figure 6 (b), indicated that the maximum voltage of the p-TEPG was the highest among the compared devices when both water and NaCl solution were utilized as energy sources. The third mechanism of the TEPG is capillary flow. When water is dropped on one side of the TEPG, a water gradient is created, and water flows between the wet and dry sides. Consequently,

the electrons in the PEDOT:PSS are electrostatically attracted to the protons and cations in the solution and are transported along the direction of solution flow, which is called pseudo-streaming current. They measured the energy generation performance of the PEDOT:PSS-coated TEPG in terms of its resistance [Figures 6 (c) and (d)]. As the resistance increased, the generated voltage increased, but the generated current decreased. Therefore, because energy density is calculated using the values of voltage and current, the appropriate resistance needs to be selected to achieve the maximum energy density [Figure 6 (e)]. Furthermore, they measured the energy harvesting performance of the TEPG by using various types of wastewaters such as sweat, rain, sewage, and seawater as the energy sources. As a result, the energy densities of all solutions were higher than that of DI water because all solutions contained salts, which enhance the difference in charge density [Figure 6 (f)]. Finally, they operated red LED lights by connecting them to the p-TEPG to demonstrate its TEPG for use in wearable devices. Since the TEPG device is a new concept of energy harvesting systems, it has not yet been researched compared to other harvesting technologies. If the research on various types of materials for TEPG devices is

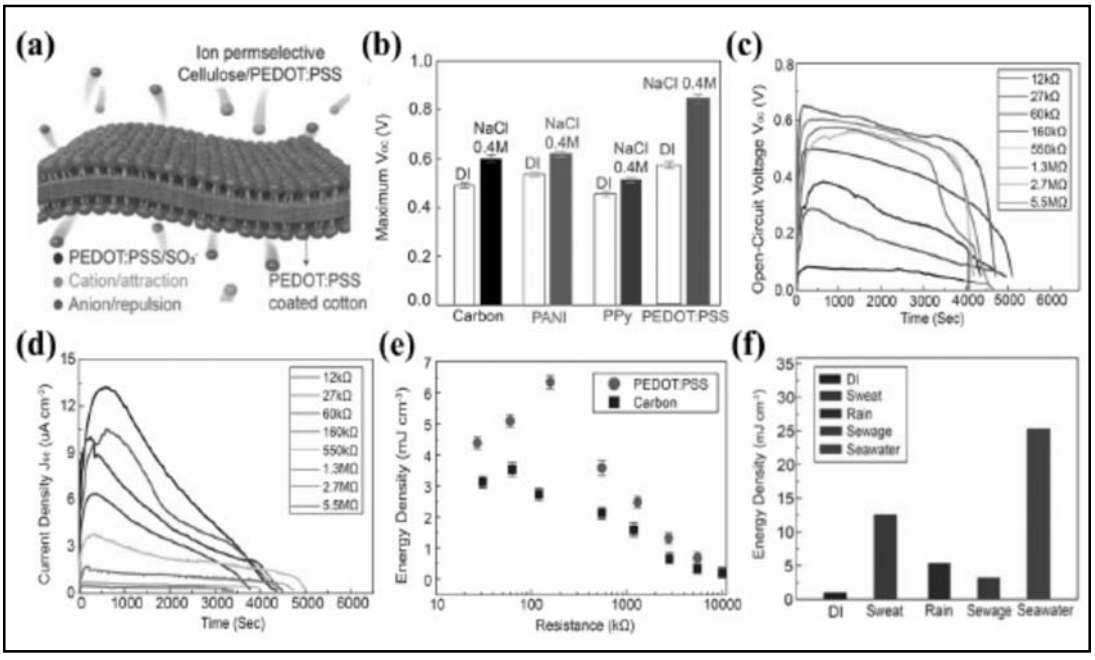

Fig. 6. (a) Schematic illustration of the ion-permselective p-TEPG system. (b) Comparison of the volumetric energy density of carbon and conducting polymer-based electrokinetic power generator. (c) Measured V_{oc} profiles by dropping 0.25 mL of DI water on various resistances of p-TEPG. (d) Measured J_{sc} profiles by dropping 0.25 mL of DI water on various resistances of p-TEPG. (e) Comparison of volumetric energy density of p-TEPG and carbon based TEPG. (f) Comparison of energy density depending on types of water. Reprinted from [48]. Copyright 2022 Elsevier.

Table 1: A summary of the PEDOT:PSS-based materials, their applications and performances

Application	Materials	Key performance	Advantages	Disadvantages	[ref]
TE	EG or DMSO treated PEDOT:PSS	Electrical conductivity (S/cm): ~620 PF ($\mu W/m \cdot K^2$): ~33	• Easy to make • Flexible • Low cost	• Very Low PF	[26]
	PEDOT:PSS/ SWCNT	Electrical conductivity (S/cm): 1000PF ($\mu W/m \cdot K^2$): 160	• High electrical conductivity, • Easy to make Flexible	• Low PF	[27]
	PEDOT:PSS / MWCNT	Electrical conductivity (S/ cm): ~654PF ($\mu W/m \cdot K^2$):133	• Easy to make • Flexible • Low cost	• Low PF	[25]
	PEDOT:PSS / graphene	Electrical conductivity (S/ cm): 637PF ($\mu W/m \cdot K^2$): 45.67	• Easy to make • Flexible • Low cost	• Very low PF	[24]
	PEDOT:PSS / Ag_2Se	Electrical conductivity (S/ cm): ~ 520PF ($\mu W/m \cdot K^2$): 327.15	• Very high PF • Easy to make • Flexible	• High cost	[30]
PV	PEDOT:PSSPEDOT: PSS /MXene	PCE : 12.4% PCE : 15.5%	• Low R_{RMS} • Large scalable	• Low PCE • High cost	[34]
	PEDOT:PSS / Brij C10	PCE : 11.2%	• Large scalable • Easy to make	• Low PCE • Rough HTL surface	[35]
	PEDOT:PSS /GO	PCE : 15%	• Large scalable • Easy to make	• Low PCE	[36]
	PEODT:PSS / CuSCN	PCE : 14.2%	• Large scalable • Easy to make	• Low PCE	[37]
Superca-pacitor	DMSO treated PEDOT:PSS	Specific capacitance: 25 F/g @ 0.1 A/g	• Easy to make	• Low specific capacitance	[44]
	rGO-diethylene glycol treated PEDOT:PSS	Maximum power density and energy density 3,589.5 W/kg and 2.83 Wh/kg	• Easy to make • Flexible • Good bending stability	-	[45]
	AC and PEDOT:PSS	Specific capacitance: 3 74 F/g @ 1 A/g	• Excellent energy storage performance • Flexible Scalable • Easy to make	-	[46]
	rGO and PEDOT:PSS	Specific capacitance: 52.2 F/ g @ 10 mV/s and 38.0 F/g @ 0.5 A/g	• Self-healable • Flexible	• Difficult to make	[47]
TEPG	PEDOT:PSS	Max. power density and energy density: 44.7 $\mu W/cm^3$ and 34.36 mJ/cm^3 (using seawater)	• Eco-friendliness • Good energy generation performance • Easy operation and fabrication	• Limited energy production with single device	[48]

conducted, TEPG devices with better energy generation can be fabricated, which is considered to be helpful for the development of flexible and wearable devices.

5. Summary and Conclusions

The summary of the applications of PEDOT:PSS-based material in energy applications are given in Table 1.

In this mini-review, the applications of PEDOT:PSS as the conductive material were summarized. The characteristics of PEDOT:PSS make it suitable for use in flexible electronic devices and effectively increase their producibility. First, PEDOT:PSS is widely used for TE due to their high Seebeck coefficient. CNT, graphene or Ag_2Se were incorporated with PEDOT:PSS to increase the PF of TE as shown in Table 1. Generally, the PEDOT:PSS-based TE showed a good flexibility and easy processability. But, there are still rooms for further enhancement of PFs. Perovskite PV was also promising applications using PEDOT:PSS. The hybrid PEDOT:PSS composites with various materials such as Mxene, graphene, or CuSCN allowed the easy and scalable production of Perovskite PV with relatively affordable PCE values. However, the perovskite PVs with PEDOT:PSS showed the relatively lower PCE than those of Si-based PVs, which requires further research on the perovskite PVs with PEDOT:PSS to enhance the PCE. Various types of supercapacitor were also studied by utilizing different types of PEDOT:PSS composites. In the applications to supercapacitors, the PEDOT:PSS contributed to the good electrochemical performances and mechanical flexible characteristics. TEPG has the attractive application areas for the next generation energy harvesting devices. TEPG using PEDOT:PSS had advantages of eco-friendliness and easiness of operation and fabrication of devices. However, the energy production capability of single TEPG devices was still limited; thus, further researches to enhance the harvesting efficiency is needed. There are constructive and continuous research on the development of various types of materials that produce synergies with PEDOT:PSS, which will overcome limitations of PEDOT:PSS in various applications. Thus, the PEDOT:PSS is expected to be positioned as a key material for futuristic electronic and energy storage/ harvesting devices.

Acknowledgement

This research was supported by the Chung-Ang University Research Scholarship Grants in 2021. This work was supported by the National Research Foundation of Korea (NRF) (No. 2022R1F1A1063696).

References

1. H. Lee, D. Lee, Y. Ahn et al., (2014). *Nanoscale,* 6: 8565-8570.
2. L. Hu, H.S. Kim, J.-Y. Lee et al., (2010). *ACS nano,* 4: 2955-2963.
3. A. Kim, Y. Won, K. Woo et al., (2013). *ACS nano, 7*: 1081-1091.
4. Z. Yu, Q. Zhang, L. Li et al., (2011). *Adv. Mater.* 23: 664-8.
5. M. Lee, Y. Ko, B.K. Min et al., (2016). *ChemSusChem,* 9: 31-5.
6. B. Hwang, Y. Han and P. Matteini, Facta Universitatis. (2022). *Series: Mechanical Engineering,* 20: 553-560.

7. C. Fragassa, Facta Universitatis. (2021). *Series: Mechanical Engineering* 19: 155-174.
8. M. Stojkovic, R. Turudija, M. Trifunovic et al., (2022). Facta Universitatis, *Series: Mechanical Engineering*.
9. Y.-M. Li, C. Deng, Z.-Y. Zhao et al., (2020). *Composites Part A: Applied Science and Manufacturing* 131.
10. W. Ren, Y. Yang, J. Yang et al., (2021). *Chemical Engineering Journal,* 415.
11. K. Nath, S. Ghosh, S.K. Ghosh et al., (2021). *Journal of Applied Polymer Science,* 138.
12. W. Gao, N. Zhao, T. Yu et al., (2020). *Carbon,* 157: 570-577.
13. J. Liang, Y. Wang, Y. Huang et al., (2009). *Carbon,* 47: 922-925.
14. G. Wang, X. Liao, F. Zou et al., (2021). *Composites Communications,* 28.
15. H. Kim, N. Qaiser and B. Hwang, (2023). *Facta Universitatis, Series: Mechanical Engineering*.
16. J.D. Ryan, D.A. Mengistie, R. Gabrielsson et al., (2017). *ACS Applied Materials & Interfaces,* 9: 9045-9050.
17. A. Lund, S. Darabi, S. Hultmark et al., (2018). *Advanced Materials Technologies,* 3: 1800251.
18. A. Lund, N.M. van der Velden, N.-K. Persson et al., (2018). *Materials Science and Engineering: R: Reports,* 126: 1-29.
19. B. Hwang and P. Matteini. (2022). *Journal of Natural Fibers,* 1-17.
20. G.B. Tseghai, D.A. Mengistie, B. Malengier et al., (2020). *Sensors, (Basel)* 20.
21. Y. Zhang, Y.J. Heo, M. Park et al., (2019). *Polymers (Basel)* 11.
22. Y. Yang, H. Deng and Q. Fu, (2020). *Materials Chemistry Frontiers* 4: 3130-3152.
23. H. Jin, J. Li, J. Iocozzia et al., (2019). *Angew Chem Int Ed Engl,* 58: 15206-15226.
24. J. Xiong, F. Jiang, H. Shi et al., (2015). *ACS Appl Mater Interfaces,* 7: 14917-25.
25. W. Lee, Y.H. Kang, J.Y. Lee et al., (2016). *RSC Advances,* 6: 53339-53344.
26. G.H. Kim, L. Shao, K. Zhang et al., (20131). *Nat Mater,* 12: 719-23.
27. C. Yu, K. Choi, L. Yin et al., (2011). *ACS nano,* 5: 7885-7892.
28. A. Kato, C. Bourges, H. Pang et al., (2022). *Polymers (Basel),* 14.
29. D. Park, M. Kim and J. Kim. (2020). *Polymers (Basel),* 12.
30. D. Park, M. Kim and J. Kim, *Polymers (Basel),* 13.
31. D. Kiermasch, L. Gil-Escrig, H.J. Bolink et al., (2019). *Joule,* 3: 16-26.
32. N.K. Tailor, M. Abdi-Jalebi, V. Gupta et al., (2020). *Journal of Materials Chemistry A,* 8: 21356-21386.
33. Y. Xia, G. Yan and J. Lin, (2021). *Nanomaterials* (Basel), 11.
34. I. Ali, M. Faraz Ud Din, D.T. Cuzzupe et al., (2022). *Molecules,* 27.
35. S. Jung, S. Choi, W. Shin *et al.,* (2023). *Polymers (Basel),* 15.
36. J. Niu, D. Yang, X. Ren et al., (2017). *Organic Electronics,* 48: 165-171.
37. L. Xu, Y. Li, C. Zhang et al., (2020). *Solar Energy Materials and Solar Cells,* 206.
38. H. Kim, A.P. Tiwari and H.Y. Kim, (2021). *Materials Today Communications,* 26.
39. X. Shi, S. Zhang, X. Chen et al., (2020). *Carbon,* 157: 55-63.
40. M. Hu, T. Hu, R. Cheng et al., (2018). *Journal of Energy Chemistry,* 27: 161-166.
41. Y. Zhang, F. Wang, H. Zhu et al., (2017). *Composites Part A: Applied Science and Manufacturing,* 101: 297-305.

42. B.R. Sankapal, H.B. Gajare, D.P. Dubal et al., (2014). *Chemical Engineering Journal,* 247: 103-110.

43. P. Anandhi, S. Harikrishnan, V.J. Senthil Kumar et al., (2022). *Electronics,* 11.

44. Y. Ko, J. Kim, D. Kim et al., (2019). *Nanomaterials (Basel),* 9.

45. Y. Liu, B. Weng, J.M. Razal et al., (2015). *Sci Rep,* 5: 17045.

46. T.G. Yun, D. Kim, S.-M. Kim et al., (2018). *Advanced Energy Materials,* 8.

47. Y. Zhao, Q. Liang, S.M. Mugo et al., (2022). *Adv Sci* (Weinh), 9: e2201039.

48. T.G. Yun, J. Bae, H.G. Nam et al., (2022). *Nano Energy,* 94.

Received: 09-12-2022

Accepted: 21-02-2023